ResearchGate

See discussions, stats, and author profiles for this publication at: https://www.researchgate.net/publication/233730930

AdsorptionÀDesorption Behavior of Cadmium(II) and Copper(II) on the Surface of Nanoparticle Agglomerates of Hydrous Titanium(IV) Oxide

ARTICLE *in* JOURNAL OF CHEMICAL & ENGINEERING DATA · JULY 2011

Impact Factor: 2.04 · DOI: 10.1021/je200222y

CITATIONS
8

READS
52

3 AUTHORS:

Sushanta Debnath
Saha Institute of Nuclear Physics
23 PUBLICATIONS **350** CITATIONS
SEE PROFILE

Debabrata Nandi
Council for Scientific and Industrial Researc…
17 PUBLICATIONS **70** CITATIONS
SEE PROFILE

Uday Chand Ghosh
Presidency University
77 PUBLICATIONS **1,302** CITATIONS
SEE PROFILE

Available from: Sushanta Debnath
Retrieved on: 02 February 2016

JOURNAL OF CHEMICAL & ENGINEERING DATA

ARTICLE

pubs.acs.org/jced

Adsorption−Desorption Behavior of Cadmium(II) and Copper(II) on the Surface of Nanoparticle Agglomerates of Hydrous Titanium(IV) Oxide

Sushanta Debnath, Debabrata Nandi, and Uday Chand Ghosh*

Department of Chemistry, Presidency University (Formerly Presidency College), 86/1 College Street, Kolkata-700073, India

ABSTRACT: The adsorption/desorption behavior of Cd^{2+} and Cu^{2+} on/from nanostructured hydrous titanium(IV) oxide (NHTO) surfaces was studied at 30 °C and pH 5.0 (± 0.1). The pseudosecond-order kinetics model described the metal ion adsorption reactions with NHTO very well ($R^2 = 1.00$). The isotherm equilibria were of a Langmuir type ($R^2_{Cd} = 1.00$, $R^2_{Cu} = 0.95$). The monolayer capacities evaluated were (0.15 and 0.46) mmol·g^{-1} for Cd^{2+} and Cu^{2+}, respectively. Investigations on the desorption of adsorbed metal ions from NHTO surfaces with a variation of complexions, ionic strength (I), and solution pH showed that ethylenediaminetetraacetic acid (EDTA; 0.01 M) and the HCl (0.1 M) solutions were the most efficient. Kinetic data of the desorption reactions between M^{2+}-NHTO (M^{2+} = Cd^{2+} or Cu^{2+}) and EDTA (0.01 M) or HCl (0.1 M) were described by the first-order equation well ($R^2 = 0.96-1.00$), except the kinetic data for the Cu^{2+} desorption by 0.01 M EDTA, which were described by the Elovich equation well ($R^2 = 0.96$). The kinetics of the desorption reactions indicated that the 0.1 M HCl could desorb metal ions from NHTO surface with more efficiency than 0.01 M EDTA. The desorption of metal ions with 0.1 M HCl could be described by an ion-exchange reaction type.

1. INTRODUCTION

Many small and large scale industries produce significant amounts of heavy metal-laden wastewater, often discharged into the environment without any prior treatment, which often is a major source of pollution and a health hazard. However, because of stringent legislation, the levels of heavy metal ions must be controlled before release to the environment,[1] as they are classified as poisons since they accumulate in living species with permanent toxic and carcinogenic effects. They are characterized by their persistence in ecosystems because of their nonbiodeterioration and their bioaccumulation along the food chain.[2] For these reasons, the presence of the heavy metal ions in the environment with concentrations not complying with pollution legislation is unacceptable, which indicates the requirement for the proper pretreatment of wastewater with recovery of metals for recycling.

Numerous technologies[3−8] have been investigated for the effective removal of toxic metals from contaminated water, such as flocculation-coagulation, precipitation, membrane-filtration, reverse osmosis, ion-exchange, and surface adsorption, and so forth. Among these, the simplest recyclable and cost-effective method is surface adsorption, because the surface can be regenerated and reused. Additionally, it requires less space for installation and produces low sludge volume. An inconvenience of the remaining processes is the production of large volumes of toxic waste or sludge that can be difficult to dispose. Therefore, an essential need is the recovery of the metal ions from the enriched waste or sludge before disposal, to prevent re-entrance of the heavy metal ions into the environment.

Therefore, recovery of metal ions from the enriched solid waste surface by desorption might be an alternative option of remediation. Again, the regenerated solid can be reused after reactivation, which should minimize the technological cost and disposal of the waste. Some workers[9−17] have made substantial efforts for the recovery of adsorbed metal ions from enriched solid surfaces by desorption. This has been carried out by the workers[9−17] mainly with the help of counter adsorption techniques and the use of some chemicals, which can replace the adsorbed substances. The use of ultrasonic sound waves has also been reported[18] for the recovery of phenol from an adsorbent surface. Desorption phenomena are now being redefined by analyzing them quantitatively using some tools to take a deeper insight into the process.[19]

The enhanced surface activity and area of nanostructured materials encouraged us to make an attempt to use these materials for scavenging undesired chemicals from contaminated water. Consequently, we synthesized nanostructured hydrous titanium(IV) oxide (NHTO) for toxic metal removal[20−22] and some mixed metal oxides[23−26] for investigating the efficiency of arsenic elimination from aqueous solution. The objectives of this present work are the optimization of reagents for the desorption of adsorbed metal ions from adsorbent surfaces to minimize the waste disposal problem. Thus, the present work reports herein the desorption behavior of adsorbed cadmium(II) and copper(II) from the agglomerated nanostructured hydrous titanium(IV) oxide (NHTO) surface.

2. MATERIALS AND METHODS

2.1. Chemicals. In this study, cadmium and copper metals (purity: 0.999) used for the preparation of stock solutions were analytical grade (A.R., BDH, England). Titanium(IV) tetrachloride (0.9950) used for the preparation of NHTO was procured from Spectrochem, India. Citric acid (CA) (0.999) and tartaric acid (TA) (0.9995) were of guaranteed reagents (G.R.) grade (Merck, India). Sodium nitrate (0.9995) and the disodium salt of

Received: October 30, 2010
Accepted: May 20, 2011
Published: June 02, 2011

ACS Publications © 2011 American Chemical Society

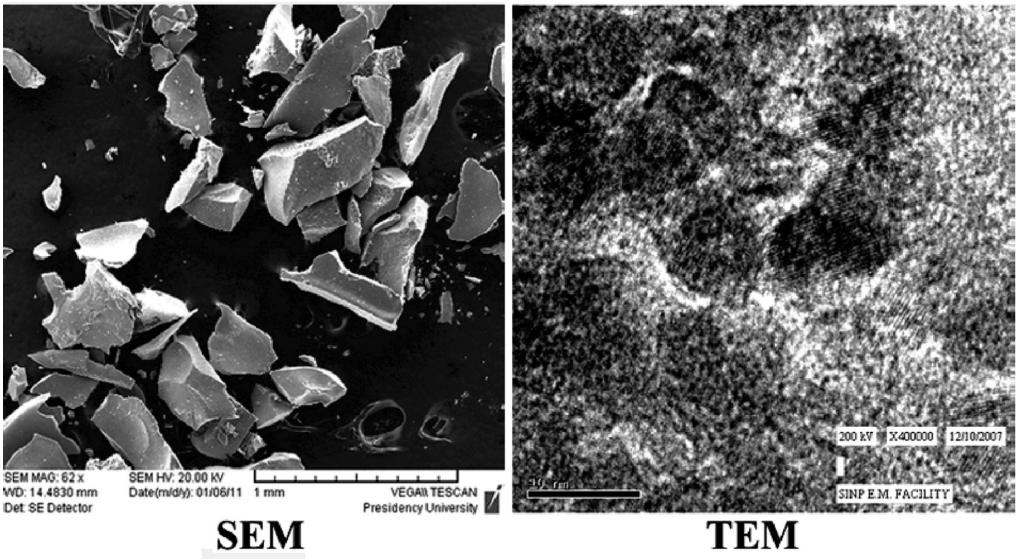

Figure 1. Scanning electron microscopic (SEM) and the transmission electron microscopic (TEM) images of NHTO.

ethylenediaminetetraacetic acid (EDTA; 0.9995) were G.R. grade (Merck, India). All other reagents used were G.R. grade (Merck, India).

2.2. Instruments. An ELICO made pH meter (model: LI-127, India) was used for the pH analysis. An atomic absorption spectrophotometer (model: AAnalyst 200, Perkin-Elmer) was used for the analysis of metal ion concentrations in the samples. A transmission electron microscopic (TEM) (FEI, Tecnai S Twin) image was taken on a copper grid at an accelerating voltage of 200 kV with attachment of a digital micrograph processor for crystallite size. A scanning electron microscope (SEM) (Tescan Vega, U.K.; model LSU+) was used for recording an image of the sample sprayed on carbon tape for surface morphology. A Quatachrome Autosorb-1C surface analyzer was used for inferring the Brunauer−Emmett−Teller (BET) surface area and pore size distribution of the material by degassing at 300 °C for 3.0 h and N_2 physisorption data at 77 K.

2.3. Metal Solution. A requisite amount of each metal was dissolved separately by treatment with 0.05 dm^3 concentrated nitric acid and diluted to 1.0 dm^3 with double-distilled water for the stock solution of metal ions (500 $mg \cdot dm^{-3}$). For the experiments, each metal solution at any desired level of concentration was made by diluting the stock solutions with double-distilled water.

2.4. Preparation of NHTO. The method used for the NHTO preparation has been described previously.[20] An outline of the procedure is given here: 0.03 dm^3 of liquid $TiCl_4$ was injected slowly into 1.0 dm^3 of well-stirred distilled water. To the milky white suspension, NH_4OH was added slowly until the pH increased to 6.4 (± 0.1). The milky white precipitate formed was aged for six days. It was filtered and washed with distilled water to make the white mass chloride-free. The white jelly mass was dried at ~80 °C in an air-oven and ground, then sieved to get the desired level of agglomerate size of the nanoparticles. The agglomerated particles ranging from (0.29 to 0.36) μm size fraction were used for the experiments.

2.5. Adsorption Experiment. For the kinetics of the adsorption reactions, 0.5 dm^3 of Cd^{2+} [initial concentration, C_0 = (2.22, 4.44, and 8.88) $\mu mol \cdot dm^{-3}$ or Cu^{2+} C_0 = (0.39, 7.86, and 15.72) $\mu mol \cdot dm^{-3}$] solutions at pH 5.0 (± 0.1) were mixed with 1.0 g of NHTO in 1.0 dm^3 glass beakers and agitated at (300 ± 10) rpm at 30 °C. At regular intervals of time, the reaction mixture was sampled (1.0 cm^3) and centrifuged. The centrifuged samples were analyzed for metal concentration. The adsorbed amount (q_{ad}, $mmol \cdot g^{-1}$) of the metal ion per gram of NHTO was calculated by eq 1.

$$q_{ad} = \frac{w_i - w_t}{m} \quad (1)$$

where w_i and w_t are the amount (mmol) of metal ion added at the beginning (t = 0) and found at any time (t) of the reaction, respectively; m is the mass (g) of NHTO added for the experiment.

For equilibrium isotherms of the adsorption reaction, to 0.05 dm^3 solution at pH = 5.0 (± 0.1) of Cd^{2+} [C_0 = (0.22 to 2.67) $mmol \cdot dm^{-3}$] or Cu^{2+} [C_0 = (0.39 to 4.72) $mmol \cdot dm^{-3}$] was added 0.1 g of NHTO in 0.25 dm^3 polyethylene bottles and agitated at a speed of (300 ± 10) rpm for an hour at temperature (T) = 30 °C. Immediately after 1.0 h of agitation, the suspended NHTO particles were separated by centrifugation, and the centrifuged solution was analyzed for metal concentrations. The adsorption capacity (q_e, $mmol \cdot g^{-1}$) of NHTO at equilibrium was calculated using eq 1, where w_t becomes w_e, the amount (mmol) of metal ion adsorbed at equilibrium.

For the preparation of metal adsorbed NHTO (M^{2+}−NHTO, where M^{2+} = Cd^{2+}/Cu^{2+}), 0.25 dm^3 of 18.0 $mmol \cdot dm^{-3}$ Cd^{2+} or 31.0 $mmol \cdot dm^{-3}$ Cu^{2+} solution (pH 5.0 ± 0.1) were taken with 5.0 g of NHTO into a 1.0 dm^3 beaker and placed in a thermostatic water bath at T = 30 °C and agitated (300 ± 10) rpm using a mechanical stirrer for 2.0 h. Once the agitation time was complete, M^{2+}-NHTO particles were separated from the liquid by filtration using a 0.45 μM membrane filter and washed with distilled water adjusted to pH 6.0 (± 0.1). Analyzing the filtrates for the Cd^{2+} or Cu^{2+} amount (q_e, $mmol \cdot g^{-1}$) adsorbed by NHTO was calculated by taking difference between the amount of metal ion taken in solution initially and found in solution at equilibrium. The metal-adsorbed NHTO (M^{2+}-NHTO) was dried overnight in an air oven at ~60 °C, which was used for the desorption experiments.

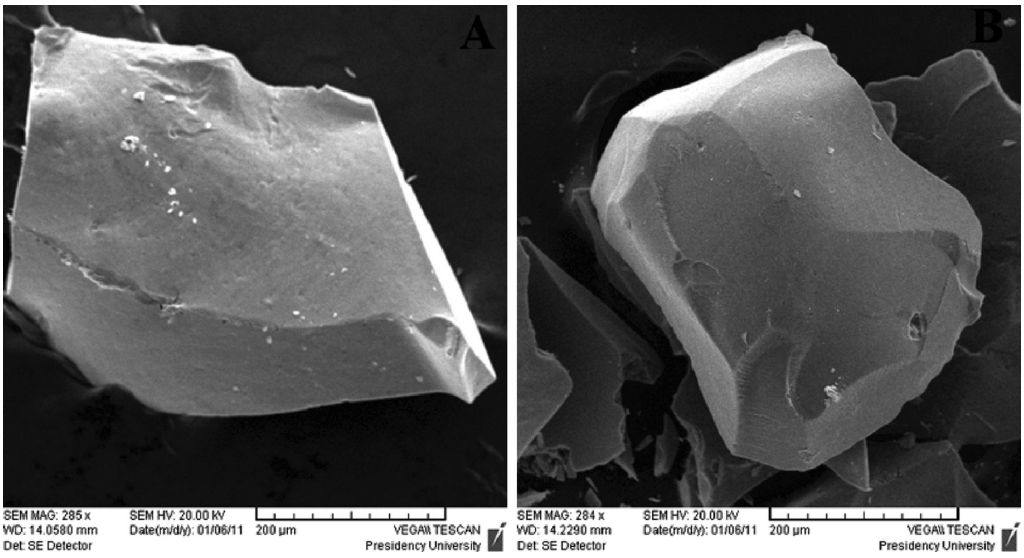

Figure 2. SEM images of (A) Cd(II)-NHTO and (B) Cu(II)-NHTO.

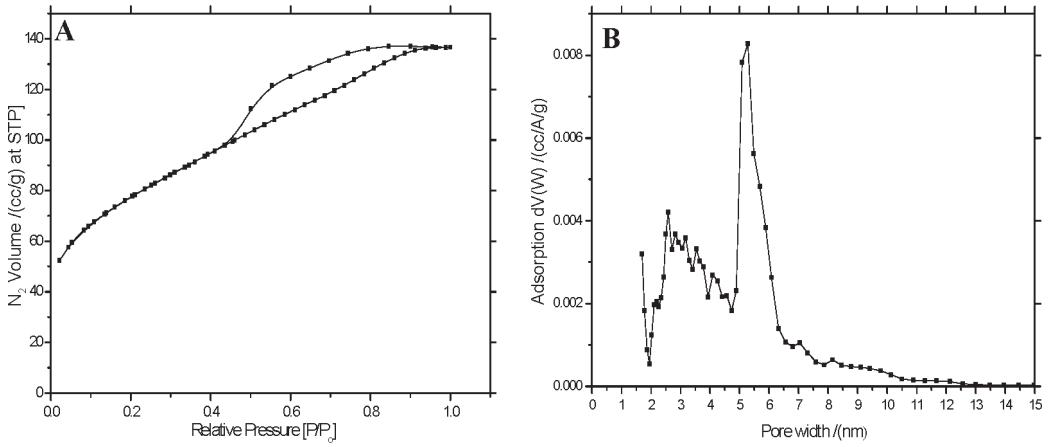

Figure 3. (A) N_2 adsorption/desorption isotherm profile and (B) pore size distribution profile of NHTO.

2.6. Desorption Experiment. For the selection of appropriate reagent for the metal ion desorption, 0.1 g of dried M^{2+}-NHTO was mixed with 0.05 dm^3 of reagent solution in the 0.25 dm^3 polyethylene bottles and agitated at (300 ± 10) rpm for 5 h. Immediately after the agitation period, the solid particles were separated using a 0.22 μM syringe filter, and the metal concentration remained in solution was analyzed by atomic absorption spectrophotometry.

For the desorption kinetics, 0.50 g of M^{2+}-NHTO was mixed with 0.50 dm^3 of the reagent solution and agitated at (300 ± 10) rpm. The sampling (1.0 cm^3) from the reaction mixture was made with variation of time from the start and analyzed for the metal ion.

3. RESULTS AND DISCUSSION

3.1. Characterization of NHTO and Metal Adsorbed NHTO. Results of the characterizations of NHTO have been reported.[20] Figure 1 shows the micrographs of the SEM and TEM images of NHTO. The SEM image showed that NHTO had irregular surface morphology. The TEM image demonstrated that NHTO was crystalline and the crystallite size was (11 to 13) nm. The X-ray diffraction pattern of NHTO[20] showed that the NHTO was crystalline with nanostructured particles. Figure 2 demonstrates the SEM images of M^{2+}-NHTO. It can be seen that the smoothness of the NHTO surface is enhanced only, which may be due to the occurrence of metal ions and the frictional effect when agitated. The parameters reported[20] were titanium content (53.4 ± 0.2) %, thermal weight loss (20.6 ± 0.2) %, bulk density (1.21 ± 0.05) g·cm^{-3}, and zero surface charge pH (pH_{zpc}) (6.5 ± 0.3). Figure 3 presents the nitrogen gas adsorption isotherm for the BET surface area analysis and the pore width distribution in NHTO. The BET surface area ($m^2 \cdot g^{-1}$) and the average pore width (nm) were 270 (± 1.5) and 5.28, respectively. The high BET surface area of NHTO agrees well with that generally expected for nanostructured materials.

3.2. Kinetics of Cd^{2+} and Cu^{2+} Adsorption Reactions. The kinetic data (q_t, mmol·g^{-1}) (not shown) for the adsorption reactions of Cd^{2+} (C_0/μmol·dm^{-3} = 22.2, 44.4, 88.8) and Cu^{2+} (C_0/μmol·dm^{-3} = 39.3, 7.86, 15.72) with NHTO obtained at T = 30 °C and pH = 5.0 (± 0.1) were analyzed by the well-known model equations[27] such as the pseudofirst-order (eq 2) and

dx.doi.org/10.1021/je200222y |J. Chem. Eng. Data 2011, 56, 3021–3028

Table 1. Kinetic Model Parameters for Cd^{2+} and Cu^{2+} Adsorption by NHTO at pH 5.0 (± 0.1) at T = 30 °C and (300 ± 10) rpm

kinetic model	kinetic parameters	$C_0 \cdot 10^2/(\text{mmol}\cdot\text{dm}^{-3})$					
		Cd(II)			Cu(II)		
		2.22	4.44	8.88	3.93	7.86	15.72
pseudofirst-order model	$k_1/(\text{min}^{-1})$	11.15 ± 0.05	8.96 ± 0.04	8.68 ± 0.03	7.73 ± 0.05	5.81 ± 0.01	4.07 ± 0.02
	q_e $(\cdot 10^2)/(\text{mmol}\cdot\text{g}^{-1})$	1.09 ± 0.002	2.17 ± 0.005	4.22 ± 0.003	1.94 ± 0.001	3.91 ± 0.002	7.46 ± 0.005
	R^2	0.93	0.96	0.99	0.99	0.99	0.96
pseudosecond - order model	$k_2/(\text{g}\cdot\text{mmol}^{-1}\cdot\text{min}^{-1})$	12.76 ± 0.05	2.37 ± 0.06	0.35 ± 0.02	6.35 ± 0.01	3.55 ± 0.03	0.57 ± 0.006
	q_e $(\cdot 10^2)/(\text{mmol}\cdot\text{g}^{-1})$	1.10 ± 0.005	2.19 ± 0.003	4.18 ± 0.002	1.89 ± 0.001	3.87 ± 0.005	7.65 ± 0.004
	R^2	1.00	1.00	1.00	1.00	1.00	1.00

Table 2. Isotherm Model Parameters Estimated for the Cd^{2+} and Cu^{2+} Adsorption Reaction with NHTO at pH 5.0 (± 0.1) at 30 °C, (300 ± 10) rpm, and 2.0 h

isotherm models	Cd(II)			Cu(II)		
Langmuir	$K_a/(\text{dm}^3\cdot\text{mmol}^{-1})$	$q_m/(\text{mmol}\cdot\text{g}^{-1})$	R^2	$K_a/(\text{dm}^3\cdot\text{mmol}^{-1})$	$q_m/(\text{mmol}\cdot\text{g}^{-1})$	R^2
	35.97 ± 0.06	0.15 ± 0.003	1.00	20.3 ± 0.04	0.46 ± 0.005	0.95
Freundlich	$K_F/(\text{mmol}\cdot\text{g}^{-1})$	n	R^2	$K_F/(\text{mmol}\cdot\text{g}^{-1})$	n	R^2
	0.18 ± 0.003	4.36 ± 0.01	0.91	0.39 ± 0.01	5.94 ± 0.05	0.85

the pseudosecond-order (eq 3) kinetic model using nonlinear statistical fit methods.

$$\text{Pseudofirst-order equation}: \log(q_e - q_t) = \log q_e - t(k_1/2.303) \quad (2)$$

$$\text{Pseudosecond-order equation}: t/q_t = 1/k_2 q_e^2 + t/q_e \quad (3)$$

where q_e and q_t are the adsorption capacities $(\text{mmol}\cdot\text{g}^{-1})$ of adsorbent, respectively, at equilibrium and time, t (min). k_1 (min^{-1}) and k_2 $(\text{g}\cdot\text{mmol}^{-1}\cdot\text{min}^{-1})$ are the pseudofirst-order and the pseudosecond-order rate constants, respectively.

The kinetic parameters estimated from the nonlinear statistical fit method of analysis of the kinetic data using the pseudofirst-order and the pseudosecond-order equations are shown in Table 1. It was found that the pseudosecond-order described the metal ion adsorption kinetic data very well (R^2 = 1.00). Again, the lowering of the k_2 value with increasing concentration of the metal solution indicated that the uptake of either metal ion by NHTO was increasingly favorable with lowering of the concentration. This is due to the fact that the positive charge on the NHTO surface has an initial rapid uptake of metal ion from the solution of high metal load, but the metal ion uptake is hindered in the later stages by the Columbic forces or lowering of the accessible active sites on the solid surface.

3.3. Equilibrium of Cd^{2+} and Cu^{2+} Adsorption Reactions. Variations of the equilibrium capacity (q_e, $\text{mmol}\cdot\text{g}^{-1}$) against the equilibrium concentration ($C_e/\text{mmol}\cdot\text{dm}^{-3}$) of Cd^{2+} ($C_0/\text{mmol}\cdot\text{dm}^{-3}$ = 0.22 to 2.67) and that of Cu^{2+} ($C_0/\text{mmol}\cdot\text{dm}^{-3}$ = 0.39 to 4.72) were analyzed separately by the most familiar isotherm equations[6,20,22] such as the Langmuir and the Freundlich isotherm models (eqs 4 and 5) (plots omitted) using a nonlinear statistical fit method to understand the nature of the active sites of the solid.

$$\text{Langmuir equation}: q_e = (q_m K_a C_e)/(1 + K_a C_e) \quad (4)$$

$$\text{Freundlich equation}: q_e = K_F C_e^{1/n} \quad (5)$$

where q_e and q_m are the equilibrium and the Langmuir monolayer adsorption capacities $(\text{mmol}\cdot\text{g}^{-1})$, K_a $(\text{dm}^3\cdot\text{mmol}^{-1})$ the Langmuir equilibrium constant; C_e is the equilibrium concentration $(\text{mmol}\cdot\text{dm}^{-3})$, and K_F $(\text{mmol}\cdot\text{g}^{-1})$ and n are the Freundlich constants.

The isotherm parameters estimated by analyzing the equilibrium data using eqs 4 and 5 are presented in Table 2. It was found that the Langmuir equation described the equilibrium data better (R^2 = 1.00 for Cd^{2+}; 0.95 for Cu^{2+}) than the Freundlich equation (R^2 = 0.91 for Cd^{2+}, 0.85 for Cu^{2+}), indicating active sites of NHTO were homogeneous and accessible equally by the metal ions. The monolayer saturation capacity (q_m, $\text{mmol}\cdot\text{g}^{-1}$) of NHTO was found to be higher for Cu^{2+} (0.46 $\text{mmol}\cdot\text{g}^{-1}$) than for Cd^{2+} (0.15 $\text{mmol}\cdot\text{g}^{-1}$), indicating that NHTO had a higher affinity for Cu^{2+} than for Cd^{2+}.

Both divalent ions should exist in aqueous solution as hydrous species[28,29] at the working solution pH 5.0 (± 0.1). The smaller Cu^{2+} (0.146 nm) ion could penetrate into the interlayer space of the adsorbent more easily than the larger Cd^{2+} (0.194 nm).[30]

The dimensionless parameter, R_L $[= (1 + C_0 K_a)^{-1}]$,[31] where K_a = the Langmuir constant $(\text{dm}^3\cdot\text{mmol}^{-1})$ and C_0 = initial concentration $(\text{mmol}\cdot\text{dm}^{-3})$ is an essential feature for predicting the isotherm type. According to Hall et al.,[31] the isotherm is (i) unfavorable for $R_L > 1.0$, (ii) linear for $R_L = 1.0$, (iii) favorable for $0 < R_L < 1.0$, and (iv) irreversible for $R_L = 1.0$. The calculation of the R_L values for adsorption of either Cd^{2+} or Cu^{2+} ions with NHTO at pH = 5.0 (± 0.1) and T = 30 °C and the C_0 range of the metal ions investigated showed the R_L values laid between zero and unity indicating the adsorption reactions were favorable.

3.4. Desorption of Metals. Desorption of either the metal ion from M^{2+}–NHTO was investigated by varying (i) complex formation ability of the metal ions with chelating reagents such as citric acid (CA), tartaric acid (TA), and the disodium salt of EDTA; (ii) concentration of H^+ derived from hydrochloric acid (HCl); (iii) influence of ionic strength of Na^+ derived from $NaNO_3$; and (iv) eluent solution pH.

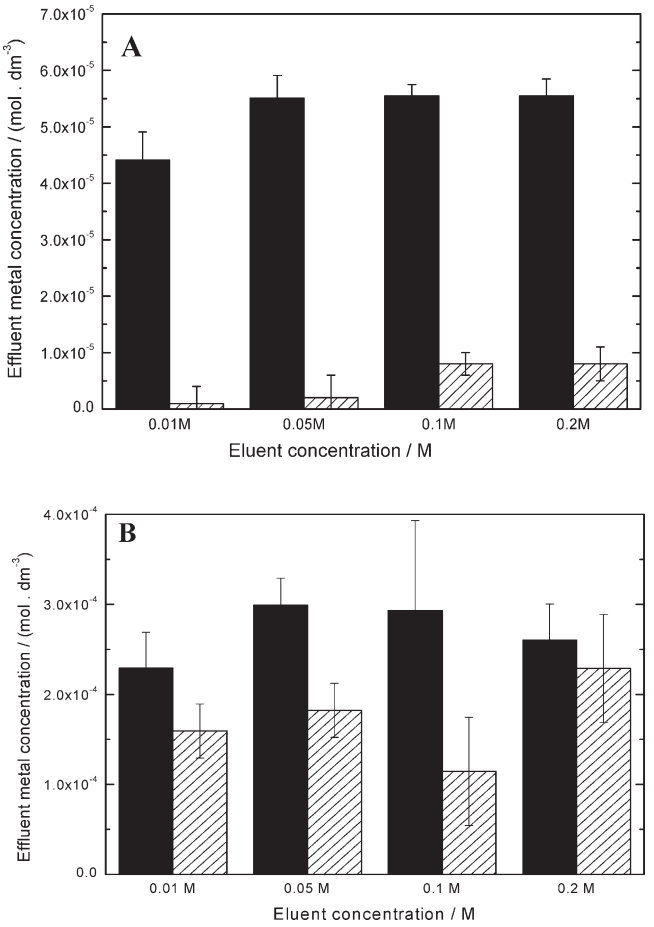

Figure 4. Effect of citric acid (CA) and tartaric acid (TA) concentrations on the (A) Cd^{2+} desorption from Cd^{2+}-NHTO (0.15 mmol $Cd^{2+}\cdot g^{-1}$) and (B) Cu^{2+} desorption from Cu^{2+}-NHTO (0.46 mmol $Cu^{2+}\cdot g^{-1}$) at T = 30 °C, (300 ± 10) rpm, and 2.0 h. Black bar: CA; striped bar: TA.

3.4.1. Effect of CA and TA Concentrations. Figure 4 parts A and B show the concentration effects of CA and TA, respectively, on the metal ion desorption from the M^{2+}-NHTO surface. It was found that the concentration of desorbed metal ions increased with increasing reagent concentration from (0.01 to 0.05) M and remained nearly constant up to 0.2 M. It was also found that the concentrations of desorbed metal ions by CA were much higher than by TA at any level of reagent concentration. This is presumably due to the fact that the solution of CA (basicity: 3) contributed a H^+ concentration higher than that of TA (basicity: 2) at a given molar concentration, which competes well for the sites of NHTO attached with metal ions. Again, the complex formation ability of CA with metal ions is greater than that of TA. Thus, the CA solution had greater metal ion desorption capability from the solid surface than TA. The concentration of CA optimized was 0.05 M for desorption of either Cd^{2+} or Cu^{2+}. However, the desorption of Cu^{2+} reduced slightly with increasing molar concentration of CA from (0.1 to 0.2) M, which might be due to the lowering of carboxylic acid group dissociation for intermolecular hydrogen bonding. Additionally, Cu^{2+} prefers to form complexes with a coordination number of four, while Cd^{2+} prefers to form complexes with a coordination number of six, indicating a lower requirement of metal-to-ligand mole ratio for complex formation with Cu^{2+} than Cd^{2+}. Thus CA could be used more efficiently than TA for desorbing metal ions from the NHTO surface.

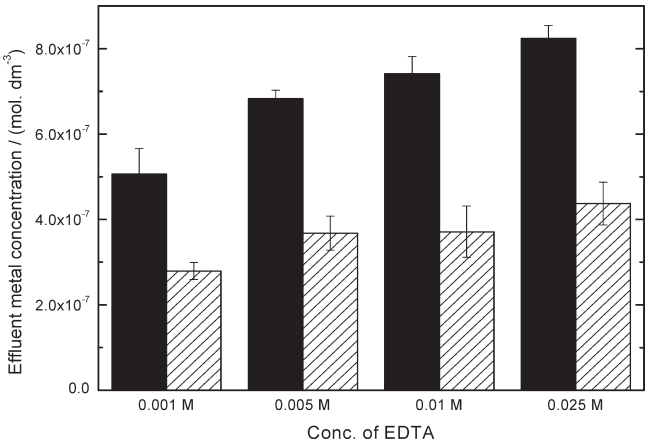

Figure 5. Effect of EDTA concentration on the desorption of Cd^{2+} and Cu^{2+} from the NHTO surface (0.15 mmol $Cd^{2+}\cdot g^{-1}$ NHTO and 0.46 mmol $Cu^{2+}\cdot g^{-1}$ NHTO) at T = 30 °C, (300 ± 10) rpm and 2.0 h. Black bar: Cu(II); striped bar: Cd(II).

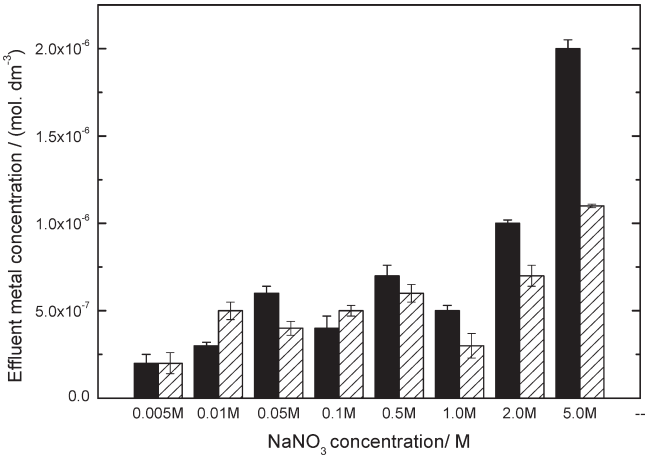

Figure 6. Effect of ionic strength ($NaNO_3$ as background salt) on the desorption of Cd^{2+} and Cu^{2+} from the NHTO surface (0.15 mmol $Cd^{2+}\cdot g^{-1}$ NHTO and 0.46 mmol $Cu^{2+}\cdot g^{-1}$ NHTO) at T = 30 °C, (300 ± 10) rpm, and 2.0 h. Black bar: Cu(II); striped bar: Cd(II).

3.4.2. Effect of EDTA Concentration. Figure 5 shows the effect of EDTA concentration on the desorption of the metal ions from M^{2+}-NHTO. It was found that the increase of molar concentration increased the concentration of the desorbed metal ions. However, the desorbed concentration of Cu^{2+} was higher than that of Cd^{2+}. This could be attributed to the fact that the smaller Cu^{2+} ion has a better ability to form complexes than the larger Cd^{2+} with EDTA because the ionic potential (charge/radius) value of Cu^{2+} is greater than that of Cd^{2+}. An increase of EDTA concentration increases the available ligand ion in solution for the abstraction of metal ions by complex formation from the solid surface, which explains the increase in desorbed metal concentration with increasing reagent solution concentration. However, the desorbed concentrations of Cu^{2+} were about twice than that of Cd^{2+}, which is again due to the higher complex formation ability of former species than the latter.

3.4.3. Effect of Ionic Strength ($NaNO_3$ as Background Salt). Figure 6 shows the effects of ionic strength of $NaNO_3$ on releasing Cd^{2+} and Cu^{2+} from M^{2+} −NHTO at a final solution of pH 5.5

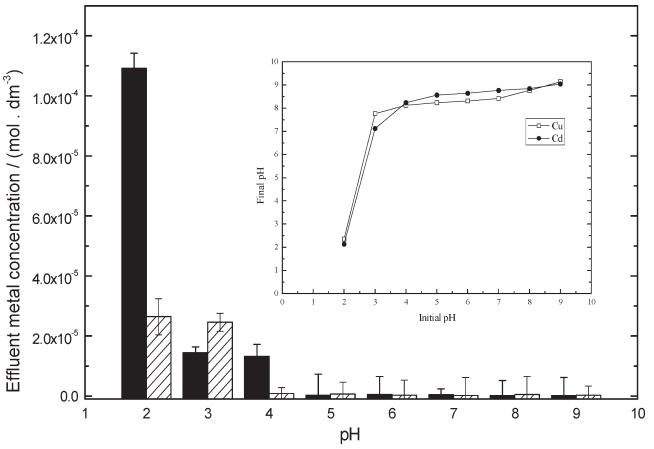

Figure 7. Effect of pH on the desorption of Cd^{2+} and Cu^{2+} from the NHTO surface (0.15 mmol $Cd^{2+}\cdot g^{-1}$ NHTO and 0.46 mmol $Cu^{2+}\cdot g^{-1}$ NHTO) at T = 30 °C, (300 ± 10) rpm, and 2.0 h. Black bar: Cu(II); striped bar: Cd(II).

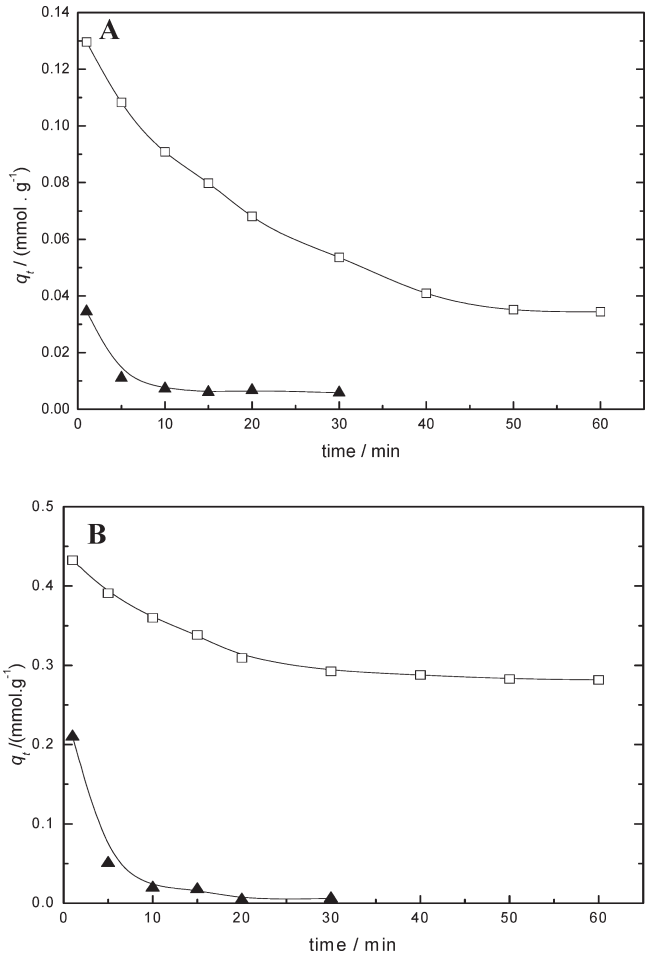

Figure 8. Kinetics of (A) Cd^{2+} desorption from Cd^{2+}-NHTO (0.15 mmol $Cd^{2+}\cdot g^{-1}$ NHTO) and (B) Cu^{2+} desorption from Cu^{2+}-NHTO (0.46 mmol $Cu^{2+}\cdot g^{-1}$ NHTO) using 0.01 M EDTA and 0.1 M HCl at T = 30 °C and (300 ± 10) rpm. □, EDTA; ▲, HCl.

(± 0.2). It was found that the concentration of desorbed metal ions increased with increasing ionic strength. It might be due to the

Table 3. Kinetic Models Used for Modeling for the Desorption of Adsorbed Cd^{2+} and Cu^{2+} from the NHTO Surface at 30 °C[a]

model	formula	eq no.
first order	$\ln(q_t) = \ln(q_\infty) - k_1 t$	6
second order	$1/q_t = 1/q_\infty + k_2 t$	7
Elovich	$q_t = (1/\beta)\ln(\alpha\beta) + (1/\beta)\ln(t)$	8
parabolic diffusion	$q_t = B + k_d t^{1/2}$	9

[a] q_t = amount of pre-adsorbed Cd^{2+} or Cu^{2+} desorbed after the desorption period (mmol·g^{-1}); k_1 = first-order desorption rate constant (min^{-1}); k_2 = second-order desorption rate constant (g·$mmol^{-1}$·min^{-1}); k_d = parabolic diffusion coefficient (mmol·$min^{1/2}$), t = time (min); q_∞ = amount of Cd^{2+} or Cu^{2+} remaining adsorbed after the desorption period (mmol·g^{-1}), α, β, B = constants of respective models.

(i) increase of Na^+ ion activity, which appears from the dissociation of $NaNO_3$ solution and competes well for the sites occupied by Cu^{2+} or Cd^{2+} on the NHTO surface; (ii) the reduction of activities of Cu^{2+} or Cd^{2+} with increasing ionic strength; and (iii) the formation of ion-pairs or chelating compounds.[32] This results in the decrease of exchangeable adsorption.[33] Additionally, the presence of background electrolytes may compress the electrical double layer surrounding the negatively charged surfaces,[34,35] which contributes to the release of adsorbed Cu^{2+} or Cd^{2+}. Most research has focused on the effect of ionic strength on the adsorption behavior of heavy metals on soils, but very little have been concerned with the desorption behavior.[36] It could be concluded that a high ionic strength is beneficial to desorption of Cu^{2+} and/Cd^{2+} from soils and to the electrokinetic removal of metal ions from contaminated soils.

3.4.4. Effect of pH on Desorption. Figure 7 shows the effect of pH on desorption of the metal ions from M^{2+}-NHTO. It was found that the desorption of metal ions increased with decreasing pH, which was found to be similar to the results that had been reported by other workers.[33−38] It might be due to the fact that (i) the high H^+ ion activity at low pH competes well for the adsorption sites that were occupied by either Cd^{2+} or Cu^{2+} ion or (ii) a change of the nature of the surface charge of NHTO at lower pH, favoring desorption of the cations. These cumulative effects facilitated the desorption of Cd^{2+} and Cu^{2+} at lower pH (≤ 4.0). The nature of solid surface becomes favorable for the adsorption at pH ≥ 5.0, and the desorption of the metal ions was very low or negligible from the M^{2+}-NHTO surface. Moreover, the precipitation of insoluble metal hydroxide might occur at higher pH values, making adsorption or desorption studies impossible. The results obtained were found to be similar with the desorption of Cd^{2+} and Cu^{2+} from soil.[39]

3.5. Kinetic Modeling of Desorption Reactions. Figure 8 parts A and B show the kinetic data of desorption reactions with 0.1 M HCl and 0.01 M EDTA, respectively. To investigate the metal ion desorption reaction rates, the data were analyzed by some standard equations[33,40−43] shown in Table 3 using the nonlinear fit method. The kinetic parameters and constants related to eqs 6 to 9 are presented in Table 4. The correlation coefficient of the kinetic parameters revealed that the metal ion desorption reaction kinetics could be described well by a first-order model (eq 6), except for the case with EDTA. It can be seen from the plots that the maximum desorption of metal ions by HCl took place in the first 10 min of each reaction. However, the desorption of the metal ions by EDTA needed a longer time to

Table 4. Kinetic Parameters and Constants with the Coefficient of Determination Values for the Desorption of Cd^{2+} and Cu^{2+} from Adsorbed NHTO at T = 30 °C and (300 ± 10) rpm

		Cd(II)		Cu(II)	
kinetic models	parameter	0.01 M EDTA	0.1 M HCl	0.01 M EDTA	0.1 M HCl
first order	k_1 ($\cdot 10^{-2}$)/min^{-1}	2.71	17.71	7.57	45.44
	q_∞ ($\cdot 10^{-4}$)/mmol·g^{-1}	1.25	0.374	4.01	3.13
	R^2	0.996	0.965	0.833	0.996
second order	k_2/g·mmol^{-1}·min^{-1}	379.912	11494.48	24.952	4628.34
	q_∞ ($\cdot 10^{-4}$)/mmol·g^{-1}	1.37	0.561	4.06	67.0
	R^2	0.970	0.829	0.780	0.943
Elovich equation	α ($\cdot 10^{-4}$)	1.41	0.303	4.43	1.68
	β ($\cdot 10^{-5}$)	−2.53	−0.849	−4.08	−5.59
	R^2	0.948	0.866	0.962	0.844
parabolic diffusion	k_d ($\cdot 10^{-5}$)/mmol·min$^{1/2}$	−1.47	−0.582	−2.28	−3.84
	B ($\cdot 10^{-4}$)	1.38	0.316	4.36	1.77
	R^2	0.973	0.660	0.900	0.642

complete. It had been seen that the desorption of Cd^{2+} and Cu^{2+} from M^{2+}-NHTO took about (50 and 30) min, respectively, to reach the maximum value. The faster desorption of Cu^{2+} than Cd^{2+} by EDTA could be attributed to the better complexion ability of Cu^{2+} than Cd^{2+}, which is due to the greater charge/radius (ionic potential) value for the former species than the latter. Thus, the abstraction of Cu^{2+} as $[Cu\text{-}EDTA]^{2-}$ was faster than Cd^{2+} as $[Cd\text{-}EDTA]^{2-}$ from M^{2+}-NHTO and increased the desorption quantity. This is evident from the higher rate constant value for the first-order process of Cu^{2+} than Cd^{2+}.

3.6. Proposed Mechanisms for the Desorption of Adsorbed Metal Ion. The results obtained best for the desorption of the metal ions were with HCl and EDTA solution. Therefore, the mechanisms proposed for the adsorption and desorption of the metal ions on and from the solid surface can be described as given below.

Adsorption at pH ∼ 5.0:

$$\text{NHTO-OH} + M^{2+} \rightarrow \text{NHTO-OM}^{+} + H^{+}$$

Desorption with HCl:

$$\text{NHTO-OM}^{+} + H^{+} \rightarrow \text{NHTO-OH} + M^{2+}$$

Desorption with H_2EDTA^{2-}:

$$\text{NHTO-OM}^{+} + H_2EDTA^{2-} \rightarrow \text{NHTO-OH} + [\text{M-EDTA}]^{2-} + H^{+}$$

Inhibition of desorption:

$$\text{NHTO-OM}^{+} + Cl^{-} \rightarrow \text{NHTO-OMCl}\ (\text{pH} > 4.0)$$

where M^{2+} stands for the Cu^{2+} or Cd^{2+} present on the NHTO surface or in aqueous solution.

Desorption by the HCl solution (pH ≤ 4.0) took place with an ion-exchange mechanism. The presence of excess H^+ ions at low pH competes well for the active sites, and desorption takes place. The Cl^- present in HCl solution at pH > 4.0 facilitated the chloro complex formation with the metal ion that exists on the NHTO surface as NHTO-OMCl, inhibiting metal ion desorption.

The H_2EDTA^{2-} forms the $[M\text{-}EDTA]^{2-}$ (M = Cd/Cu) complex, and the metal ions being adsorbed on the surface are desorbed from the sites. Desorption with HCl is an acid−base exchange type reaction, and thus it was very fast, which is reflected in the values of the desorption rate constants.

4. CONCLUSION

Adsorption−desorption behaviors of Cu^{2+} and Cd^{2+} were investigated separately using NHTO. The kinetics of the adsorption reactions at optimized pH (5.0 ± 0.1) was described by a pseudosecond-order equation well. The equilibrium of metal ion adsorption reactions with NHTO at 30 °C obeyed the Langmuir isotherm. Desorption investigations of the metal ions from the solid surface separately by CA, TA, EDTA, ionic strength, and solution pH showed that 0.01 M EDTA and 0.1 M HCl were the best possible reagents. Desorption kinetics investigated using EDTA and HCl were described well by a first-order kinetic equation except for Cu^{2+} desorption by 0.01 M EDTA. The desorption of Cu^{2+} by 0.01 M EDTA was explained by the Elovich model. The highest ionic strength and lowest solution pH showed good desorption capability of metal ions from M^{2+}-NHTO. Again, the efficiency of HCl (0.1 M) is greater than that of EDTA (0.01 M). The desorption of metal ions by HCl took place with an ion-exchange mechanism. The reaction of H^+ with M^{2+}-NHTO is an acid−base type and very fast, which is reflected from the high desorption rate. The desorption of metal ions with EDTA by complex formation was slow for the heterogeneous phase reaction.

AUTHOR INFORMATION

Corresponding Author
*E-mail: ucghosh@yahoo.co.in.

ACKNOWLEDGMENT

The authors are grateful to the Vice Chancellor and Head, Department of Chemistry, Presidency University for providing the laboratory facilities. Also the authors are grateful to the Head, Department of Geology, Presidency University for helping with the scanning electron microscopic images of the samples.

REFERENCES

(1) Wang, L. K.; Yang-Tse, H.; Lo, H.; Yapijakis, C. *Waste Treatment in Food Processing Industry*; Taylor & Francis Group: Boca Raton, FL, 2006; Chapter 1.

(2) Sitting, M. *Handbook of Toxic and Hazardous Chemicals*; Noyes Publications: Park Ridge, NJ, 1981.

(3) Mustafa, S.; Waseem, M.; Naeem, A.; Shah, K. H. Selective Sorption of Cadmium by Mixed Oxides of Iron and Silicon. *Chem. Eng. J.* **2010**, *157*, 18–24.

(4) Naeem, A.; Fein, J. B.; Woertz, J. R. Experimental Measurement of Proton Cd, Pb, Sr and Zn Adsorption onto Fungal Species Saccharomyces Cerevisiae. *Environ. Sci. Technol.* **2006**, *40*, 5724–5729.

(5) Naeem, A.; Westerhoff, P.; Mustafa, S. Vanadium Removal by Metal (Hydr)oxide Adsorbents. *Water Res.* **2007**, *41*, 1596–1602.

(6) Bhattacharya, A. K.; Naiya, T. K.; Mandal, S. N.; Das, S. K. Adsorption, Kinetics and Equilibrium Studies on Removal of Cr(VI) from Aqueous Solutions Using Different Low-Cost Adsorbents. *Chem. Eng. J.* **2008**, *137*, 529–541.

(7) Mustafa, S.; Waseem, M.; Naeem, A.; Shah, K. H.; Ahmad, T. Cd^{2+} ion Removal Silica, Iron hydroxide and their Equilimolar Mixed Oxide from Aqueous Solution. *Desalination* **2010**, *255*, 148–153.

(8) Safdar, M.; Mustafa, S.; Naheem, A.; Mahmod, T.; Waseem, M. Effect of Sorption on Co(II), Cu(II), Ni(II) and Zn(II) precipitation. *Desalination* **2011**, *266*, 171–174.

(9) Vilar, V. J. P.; Botelho, C. M. S.; Boaventura, R. A. R. Copper desorption from Gelidium algal biomass. *Water Res.* **2007**, *41*, 1569–1579.

(10) Mustafa, G.; Kookana, R. S.; Singh, B. Desorption of cadmium from goethite: Effects of pH, temperature and aging. *Chemosphere* **2006**, *64*, 856–865.

(11) Yuan, S.; Xi, Z.; Jiang, Y.; Wan, J.; Wu, C.; Zheng, Z.; Lu, X. Desorption of copper and cadmium from soils enhanced by organic acids. *Chemosphere* **2007**, *68*, 1289–1297.

(12) Wang, S.; Nan, Z.; Zeng, J.; Hu, T. Desorption of zinc by the kaolin from Suzhou, China. *Appl. Clay Sci.* **2007**, *37*, 221–225.

(13) Shan, X.; Lian, J.; Wen, B. Effect of organic acids on adsorption and desorption of rare earth elements. *Chemosphere* **2002**, *47*, 701–710.

(14) Zhu, L. Q.; Yuan, C. L.; Jing, Z.; Hui, Y. Z.; Wei, W. Q. Lead desorption from modified spent grain. *Trans. Nonferrous Met. Soc. China* **2009**, *19*, 1371–1376.

(15) Martins, B. L.; Cruz, C. C. V.; Luna, A. S.; Henriques, C. A. Sorption and desorption of Pb^{2+} ions by dead *Sargassum* sp. Biomass. *Biochem. Eng. J.* **2006**, *27*, 310–314.

(16) Min, K.; Hua, Y. G.; Jun, C. W.; Zhang, Z. X. Study on mercury desorption from silver-loaded activated carbon fibre and activated carbon fibre. *J. Fuel Chem. Technol.* **2008**, *36*, 468–473.

(17) Wang, D. Z.; Jiang, X.; Rao, W.; He, J. Z. Kinetics of soil cadmium desorption under simulated acid rain. *Ecol. Complex* **2009**, *6*, 432–437.

(18) Li, Z.; Xu, K.; Li, X.; Xi, H.; Hua, B.; Li, F. Effect of ultrasound on desorption kinetics of phenol from polymeric resin. *Ultrason. Sonochem.* **2006**, *13*, 225–231.

(19) Kanervo, J. M.; Keskitalo, T. J.; Slioor, R. I.; Krause, A. O. I. Temperature-programmed desorption as a tool to extract quantitative kinetic or energetic information for porous catalysts. *J. Catal.* **2006**, *238*, 382–393.

(20) Debnath, S.; Ghosh, U. C. Nanostructured hydrous titanium(IV) oxide: Synthesis, characterization and Ni(II) adsorption behaviour. *Chem. Eng. J.* **2009**, *152*, 480–491.

(21) Debnath, S.; Biswas, K.; Ghosh, U. C. Removal of Ni(II) and Cr(VI) with Titanium(IV) Oxide Nanoparticle Agglomerates in Fixed-Bed Columns. *Ind. Eng. Chem. Res.* **2010**, *49*, 2031–2039.

(22) Debnath, S.; Ghosh, U. C. Equilibrium modelling of single and binary adsorption of Cd(II) and Cu(II) onto agglomerated nano structured titanium(IV) oxide. *Desalination* **2011**, *273*, 330–342.

(23) Gupta, K.; Saha, S.; Ghosh, U. C. Synthesis and characterization of nanostructure hydrous iron-titanium binary mixed oxide for arsenic sorption. *J. Nanopart. Res.* **2008**, *10*, 1361–1368.

(24) Gupta, K.; Biswas, K.; Ghosh, U. C. Nanostructure iron(III)-zirconium(IV) binary mixed oxide: synthesis, characterization and physicochemical aspects of arsenic(III) sorption from the aqueous solution. *Ind. Eng. Chem. Res.* **2008**, *47*, 9903–9912.

(25) Gupta, K.; Maity, A.; Ghosh, U. C. Manganese associated nanoparticle agglomerate of iron(III) oxide: synthesis, characterization and arsenic(III) sorption behavior with mechanism. *J. Hazard. Mater.* **2010**, *184*, 832–842.

(26) Basu, T.; Ghosh, U. C. Synthesis, characterization and arsenic-(V) adsorption in the presence of groundwater co-occurring ions on nanostructured iron(III)-chromium(III) bimetal mixed oxide. *Water Qual. Res. J. Can.* **2010**, in press.

(27) Ho, Y.-S. Review of second-order models for adsorption systems. *J. Hazard. Mater.* **2006**, *B136*, 681–689.

(28) Arias, M.; Novo, C. P.; Osorio, F.; López, E.; Soto, B. Adsorption and desorption of copper and zinc in the surface layer of acid soils. *J. Colloid Interface Sci.* **2005**, *228*, 21–29.

(29) Srivastava, P.; Singh, B.; Angove, M. Competitive adsorption behaviour of heavy metals on kaolinite. *J. Colloid Interface Sci.* **2005**, *290*, 28–38.

(30) He, H. P. *Studies on the Interaction of Clayed Mineral and Metallic Ions*; Petrolic Industrial Press: Beijing, 2001.

(31) Hall, K. R.; Eagleton, L. C.; Acrivos, A.; Vermulent, T. Pore and solid diffusion kinetics in fixed-bed adsorption under constant pattern conditions. *Ind. Eng. Chem. Fundam.* **1966**, *5*, 212.

(32) Chen, H. M. *Heavy Metal Pollution in Sol-Plant System*; Science Press: Beijing, 1996.

(33) Undabeytia, T.; Nir, S.; Tytwo, G.; Serban, C.; Morillo, E.; Maqueda, C. Modeling adsorption−desorption processes of Cu on edge and planar sites of montmorillonite. *Environ. Sci. Technol.* **2002**, *36*, 2677–2683.

(34) Phillips, I. R.; Lamb, D. T.; Warker, D. W.; Burton, E. D. Effect of pH and salinity on copper, lead, and zinc sorption rates in sediments from Moreton bay, Australia. *Bull. Environ. Contam. Toxicol.* **2004**, *73*, 1041–1048.

(35) Xu, Y. H.; Zhao, D. Y. Removal of copper from contaminated soil by use of poly(amidoamine) dendrimers. *Environ. Sci. Technol.* **2005**, *39*, 2369–2375.

(36) Gao, Y.; Kan, A. T.; Tomson, M. B. Critical evaluation of desorption phenomena of heavy metals from natural sediments. *Environ. Sci. Technol.* **2003**, *37*, 5566–5573.

(37) Puls, R. W.; Powell, R. M.; Donald, C.; Eldred, C. J. Effect of pH, solid/solution rate, ionic strength, and organic acids on Pb and Cd sorption on kaolinite. *Water, Air, Soil Pollut.* **1991**, *57−58*, 423–430.

(38) Ören, A. H.; Kaya, A. Factors affecting adsorption characteristics of Zn^{2+} on two natural zeolites. *J. Hazard. Mater.* **2006**, *131*, 59–65.

(39) Yuan, S.; Xi, Z.; Jiang, Y.; Wan, J.; Wu, C.; Zheng, Z.; Lu, X. Desorption of copper and cadmium from soils enhanced by organic acids. *Chemosphere* **2007**, *68*, 1289–1297.

(40) Xu, R. K.; Yua, G.; Kozak, L. M.; Huang, P. M. Desorption kinetics of arsenate adsorbed on Al (oxy)hydroxides formed under the influence of tannic acid. *Geoderma* **2008**, *148*, 55–62.

(41) Saha, U. K.; Liu, C.; Kozak, L. M.; Huang, P. M. Kinetics of selenite desorption by phosphate from hydroxyaluminum- and hydroxyaluminosilicate- montmorillonite complexes. *Geoderma* **2005**, *124*, 105–119.

(42) Wang, D. Z.; Jiang, X.; Rao, W.; He, J. Z. Kinetics of soil cadmium desorption under simulated acid rain. *Ecol. Complex* **2009**, *6*, 432–437.

(43) Li, D.; Huang, S.; Wang, W.; Peng, A. Study on the kinetics of cerium(III) adsorption-desorption on different soils in China. *Chemosphere* **2001**, *44*, 663–669.